remote sensing

MDPI

Article

Assessment of Bottom-Up Satellite Precipitation Products on River Streamflow Estimations in the Peruvian Pacific Drainage

Jonathan Qquenta [1,2,*], Pedro Rau [3], Luc Bourrel [4], Frédéric Frappart [5] and Waldo Lavado-Casimiro [2]

[1] Master's Program in Hydraulic Engineering, Postgraduate Unit, Faculty of Physical Sciences, Universidad Nacional Mayor de San Marcos (UNMSM), Av. Carlos Germán Amezaga 375, Lima 15081, Peru
[2] National Service of Meteorology and Hydrology of Peru (SENAMHI), Lima 15072, Peru; wlavado@senamhi.gob.pe
[3] Water Research and Technology Center (CITA), Department of Civil and Environmental Engineering Universidad de Ingeniería y Tecnología (UTEC), Lima 15063, Peru; prau@utec.edu.pe
[4] UMR 5563 Géosciences Environnement Toulouse (GET), Université de Toulouse, CNRS, IRD, UPS, CNES, OMP, 14 Avenue Edouard Belin, 31400 Toulouse, France; luc.bourrel@ird.fr
[5] Interactions Sol Plante Atmosphère (ISPA), UMR 1391 Institut National de Recherche pour l'Agriculture, Alimentation et l'Environnement (INRAE)/Bordeaux Science Agro, 33140 Villenave-d'Ornon, France; frederic.frappart@inrae.fr
* Correspondence: jonathan.qquenta@unmsm.edu.pe; Tel.: +51-947-714-001

Abstract: In regions with limited precipitation information, like Peru, many studies rely on precipitation data derived from satellite products (SPP) and model reanalysis. These products provide near-real-time information and offer global spatial coverage, making them attractive for various applications. However, it is essential to consider their uncertainties when conducting hydrological simulations, especially in a key region like the Pacific drainage (Pd), where 56% of the Peruvian population resides (including the capital, Lima). This study, for the first time, assessed the performance of two bottom-up Satellite-based Precipitation Products (SPP), GPM + SM2RAIN and SM2RAIN-ASCAT, and one top-down approach SPP, ERA5-Land, for runoff simulation in the Pacific drainage of Peru. Hydrological modeling was conducted on 30 basins distributed across the Pd, which were grouped into 5 regions (I–V, ordered from south to north). The results showed that SM2RAIN-ASCAT performed well in regions I-III-IV, ERA5-Land in region II, and GPM + SM2RAIN in region V. The hydrological model GR4J was tested, and better efficiency criteria were obtained with SM2RAIN-ASCAT and GPM + SM2RAIN when comparing the simulated versus observed streamflows. The hydrological modeling using SM2RAIN-ASCAT and GPM + SM2RAIN demonstrated satisfactory efficiency metrics (KGE > 0.75; NSE > 0.65). Additionally, ten hydrological signatures were quantified to assess the variability of the simulated streamflows in each basin, with metrics such as Mean Flow (Q mean), 5th Quantile Flow (Q5), and 95th Quantile Flow (Q95) showing an overall better performance. Finally, the results of this study demonstrate the reliability of using bottom-up satellite products in Pd basins.

Keywords: daily discharge; ERA5-Land; GPM + SM2RAIN; GR4J; hydrological model; Peruvian Pacific drainage; precipitation satellite products; SM2RAIN-ASCAT

Citation: Qquenta, J.; Rau, P.; Bourrel, L.; Frappart, F.; Lavado-Casimiro, W. Assessment of Bottom-Up Satellite Precipitation Products on River Streamflow Estimations in the Peruvian Pacific Drainage. *Remote Sens.* **2024**, *16*, 11. https://doi.org/10.3390/rs16010011

Academic Editor: Yuriy Kuleshov

Received: 3 October 2023
Revised: 9 December 2023
Accepted: 11 December 2023
Published: 19 December 2023

1. Introduction

Precipitation is considered to be the most important variable in geosciences [1] due to its nature of being the main input in the hydrological cycle, as well as its application in the design of hydraulic structures, natural disaster management, weather forecasting, agricultural planning, and among other fields [2,3]. Furthermore, due to climate change, the frequency and intensity of climatic extremes will increase, with meteorological variables such as precipitation being particularly affected [4]. This, in turn, will lead to an increase

in the number and intensity of droughts (precipitation scarcity) and floods (increased precipitation) [5], with direct impacts on ecosystem functioning [6] and risk management [7]. In this context, it is essential to assess precipitation, whether from observed stations or satellite products, to significantly enhance water resource management and environmental management, among other aspects.

However, the spatio-temporal monitoring of precipitation with an extensive network of ground measurement stations across a territory is crucial [8], but is scarce in developing countries, such as Peru. In recent years, various alternatives have been presented to overcome the scarcity of precipitation data, including meteorological models, radars, etc. [9]. Therefore, the estimation of satellite-based precipitation products (SPP) has emerged as a comprehensive and viable source of information, offering global coverage and mostly being freely accessible [10,11]. Some of the most widely used satellite products worldwide are the Tropical Rainfall Measuring Mission (TRMM), Climate Hazards Group InfraRed Precipitation with Station data (CHIRPS), and Global Precipitation Measurement Mission (GPM), among others [9,12]. These satellite products provide global coverage, spatial resolution in the range of 5–25 km, and temporal resolution ranging from hourly to daily and monthly, with some datasets extending from 1950 to the present.

These SPP typically estimate precipitation based on cloud properties (top-down approach). However, recent developments propose a novel approach that involves estimating precipitation from soil moisture, known as the bottom-up approach [13]. Bottom-up products, such as SM2RAIN-ASCAT and GPM + SM2RAIN, stand out due to their high spatiotemporal resolution, accurately capturing local patterns and leveraging soil moisture to estimate precipitation in data-scarce areas [14,15]. Furthermore, they provide global and open access data, and are, hence, beneficial for hydrological applications and water resources management [15]. However, they exhibit weaknesses related to uncertainty in the soil–precipitation relationship, dependence on hydrological models, and sensitivity to soil conditions. In contrast, top-down products, such as TRMM or model reanalysis output s, like ERA5-Land, rely on observations from various sources to estimate precipitation and are integrated into complete climate systems, providing a global perspective. Although they are adjusted on in-situ observation records and employed as inputs and in many models, they face challenges in areas with limited access, high uncertainty in sparsely observed regions, and potential errors due to simplifications in atmospheric physics [13]. Additionally, it is noted that reanalysis products like ERA5-Land have the capability to assimilate information from new stations and data, resulting in a significant increase in the amount of collected and generated information [2,16]. While this can bring benefits as more up-to-date records could be obtained, it may also introduce uncertainty due to the reliability and control of the required data. Thus, the quality and quantity of the available data vary over time and in different regions, which can affect the accuracy of the precipitation estimates and, consequently, the hydrological outcomes based on these products.

Furthermore, it is described that the main difference between the two approaches lies in the object of measurement. While the top-down approach estimates instantaneous precipitation rates, the bottom-up approach estimates accumulated precipitation rates. Among the bottom-up SPP, SM2RAIN-ASCAT and GPM + SM2RAIN are presented as some of the most recent products based on soil moisture, both available at a daily resolution with global coverage, multiple versions, and data availability since 2007 [10,11].

SPP are applied in basins worldwide due to their global coverage and complete precipitation records covering a relatively long period. However, these benefits do not eliminate the uncertainties related to their generation [17], which also is presented in applications such as hydrological modeling. While SPP, when possible, are compared and adjusted with ground-based stations, they should also be evaluated for their ability to generate streamflows [18]. While, at present, there are innovative methods for estimating daily streamflow [19], this article utilizes traditional approaches for streamflow generation, such as hydrological models. However, this does not rule out the potential to generate daily streamflows using new and improved methodologies [20].

Hence, the major challenges lie in the conditions under which SPP are obtained and/or generated, as well as in the effective integration of these two approaches in applications as top-down products are based on climate models and global observations, while bottom-up products rely on hydrological models and soil moisture data [14,21,22]. The heterogeneity of the data and differences in the spatial and temporal scales between the approaches raise challenges in synchronizing and calibrating hydrological models. Another challenge in using SPP for streamflow generation is the validation of hydrological models, as different performance statistics are employed, such as the Nash-Sutcliffe Efficiency (NSE) and Kling-Gupta Efficiency (KGE), among others [2,8]. These criteria allow for evaluating the degree of agreement between streamflows simulated by a hydrological model. Some studies have found that bottom-up products, such as SM2RAIN-ASCAT and GPM + SM2RAIN, exhibit relatively high KGE values compared to other precipitation products, indicating a good performance in replicating observed streamflows.

In Peru, the limited network of hydrometeorological stations hinders the study of ungauged basins [1,15,23,24]. As a result, various studies have employed Satellite-based Precipitation Products (SPP) with the traditional top-down approach in various engineering applications. However, since the formulation of the bottom-up approach, several authors have indicated that in many locations, this innovative approach has outperformed the top-down approach in replicating observed streamflows [18]. Hence, the novelty and objective of this article lie in assessing, for the first time, bottom-up SPP in the Pacific drainage (Pd) and demonstrating the advantages of this approach over the traditional top-down approach for streamflow generation in Peruvian basins.

This study is focused on the Pacific drainage (Pd) due to its high population density, the presence of major irrigation projects, reservoirs, and its diverse climatic and hydrological characteristics. Due to it being a region of interest, authors have carried out studies on the Pd runoff [25], and drought events have also been evaluated in the Pd [26].

After verifying the potentialities of the bottom-up approach in the Pacific drainage (Pd), the possibility of its application in all engineering-related aspects of water resources emerges. These aspects include hydrological studies, peak flow analyses, and water balance assessments, among others, consequently enhancing water and environmental management. Another innovation of the study is the utilization of 10 hydrological signatures and statistical metrics such as Skill Score (SS) for a more robust evaluation of the results. In addition, the study conducted spatial comparisons (between regions) and assessed the performance based on the watershed size, among other factors. Finally, given the limited availability of information in certain locations, bottom-up SPP are presented as a viable alternative to serve as meteorological forcing, thereby generating streamflows. The study also suggests that a detailed assessment of the performance of these products in different regions of the watershed will help to identify their strengths and limitations, contributing to improving the accuracy of hydrological simulations and providing valuable information for water management in the area.

2. Materials

2.1. Study Area

Peru covers an area of 1,285,216 km^2 and is divided into three major hydrographic regions: Pacific, Amazonian, and Titicaca, where Pacific drainage (Pd) covers 278,482 km^2, representing 21.7%. The Pd accommodates nearly 56% of the country's total population, including the capital, Lima, with more than 10 M people, exhibiting high spatial demographic variability across the steep slopes and a high risk to water stress and flood prone areas [27]. This study evaluated 30 basins distributed in the Pd, which were grouped into 5 regions, as determined by the Peruvian Administrative Water Authorities (AAA) [28] (Figure 1a). Basin sizes vary in a range of between 400 and 17,000 km^2. They are delimited with respect to a hydrometric station. Regions I, II, III, IV, and V, defined by AAA, encompassed 5, 2, 12, 5, and 7 basins, respectively (Table 1). Figure 1a also shows the extent and spatial location of the 30 analyzed basins. In this way, the basins in southern and central regions (I to III) are

at an altitude higher than 3500 msl, while the basins in northern regions (IV-V) culminate at an altitude ranging between 2500 and 3500 msl.

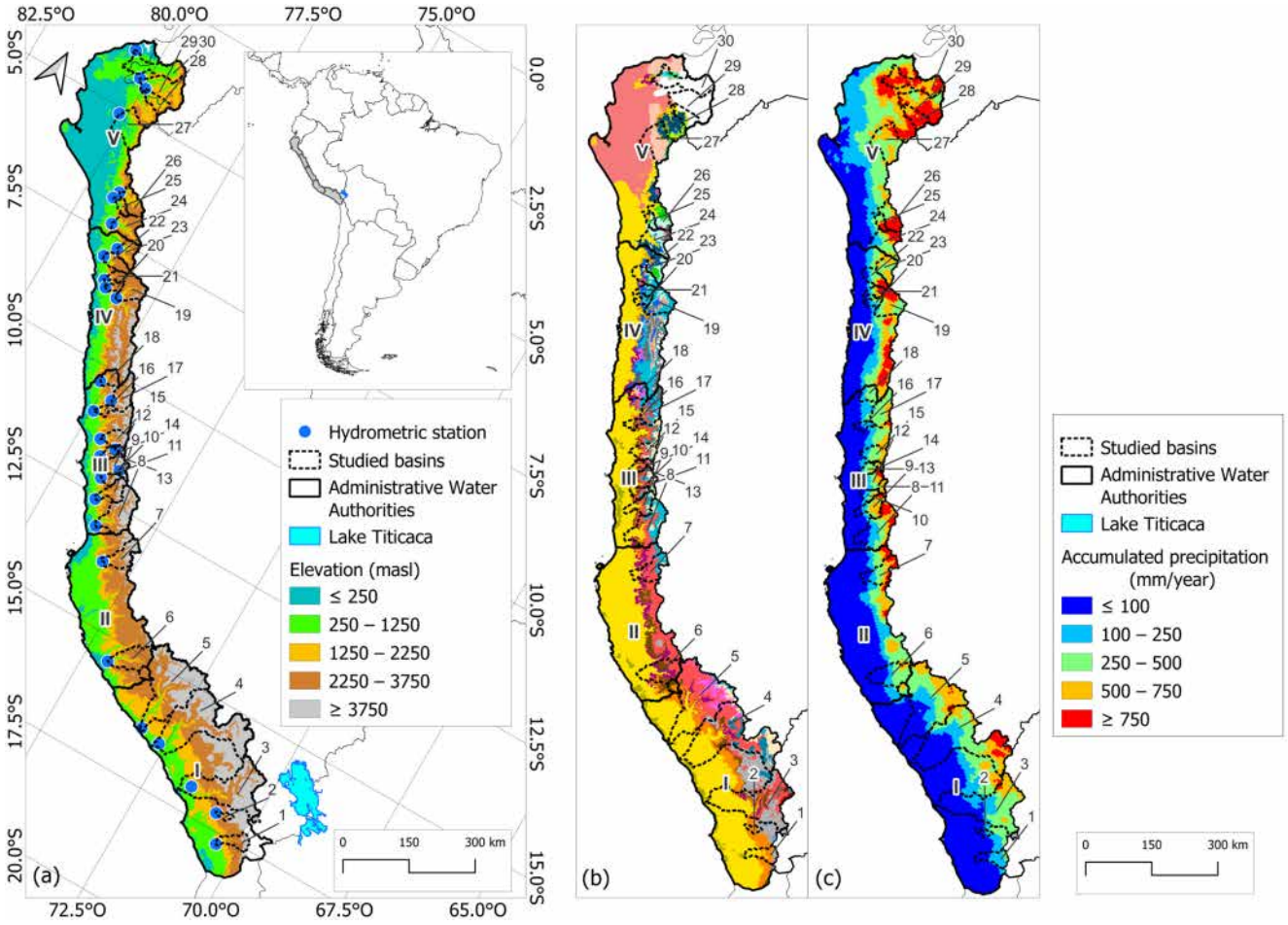

Figure 1. (**a**) Map of location and elevation of the 30 basins along the Pacific drainage (Pd). Discretization of the Pd into 5 studied regions (Region I: Caplina-Ocoña; Region II: Chaparra Chincha; Region III: Cañete-Fortaleza; Region IV: Huarmey-Chicama; Region V: Jequetepeque-Zarumilla; (**b**) Climate classification map (see full legend in [29]) developed by SENAMHI along the Pacific drainage and (**c**) Multi-year average cumulative precipitation map in the Pacific drainage basin created from SENAMHI's PISCO data [30] over 38 years (1981–2018).

The study area, due to its territorial extension, presents 33 of the 38 climatic zones identified in the Climate Classification Map of Peru developed by the National Service of Meteorology and Hydrology of Peru (SENAMHI) [29], with the remaining 5 climates found in the Amazonian and Titicaca.

Predominantly, throughout the entire Pacific drainage, there is an arid and temperate climate (Figure 1b). Thus, in regions I, II, III, and IV, a climate typified with code E (d) B (yellow) predominates, described as "Arid with moisture deficiency in all seasons of the year-Temperate". In region V, a climate typified with code E (d) A (pink) prevails, described as "Arid with moisture deficiency in all seasons of the year-Warm". Additionally, on the Pacific drainage, the predominant vegetation cover and land use are coastal and Andean agriculture and lithic leptosol-lithic outcrop soils, respectively.

On the other hand, Figure 1c displays the annual cumulative precipitation distributed along the Pacific drainage. It is noteworthy that the highest precipitation values are mainly found in the upper parts of the basins. Also, in the lower parts of the basins near the Pacific Ocean, the lowest cumulative precipitations are recorded (<100 mm/year).

Table 1. Distribution of the 30 basins in the Pacific drainage (Pd).

Region (AAA)	ID	Hydrometric Station	Basin	Flow (mm/day)	Area (km^2)
Region I: Caplina-Ocoña	1	La Tranca	Sama	2.16	1937
	2	Tumilaca	Ilo-Moquegua	0.91	462
	3	La Pascana	Tambo	13.7	13,020
	4	Huatipa	Camaná	71.8	16,937
	5	Ocoña	Ocoña	95.08	16,029
Region II: Chaparra-Chincha	6	Yauca	Yauca	5.47	4113
	7	Letrayoc	Pisco	41.79	3079
Region III: Cañete-Fortaleza	8	Socsi	Cañete	46.16	5786
	9	La Capilla	Mala	13.48	2145
	10	Antapucro	Lurín	6.74	996
	11	Tamboraque	Rímac	15.31	576
	12	Chosica	Rímac	1.24	2305
	13	Puente Magdalena	Chillón	0.47	1246
	14	Obrajillo	Chillón	5.74	365
	15	Santo Domingo	Chancay-Huaral	17.07	1835
	16	Las Minas	Supe	8.49	766
	17	Cahua	Pativilca	38.01	2949
	18	Malvados	Chicama	10.65	1378
Region IV: Huarmey-Chicama	19	Condorcerro	Santa	143.43	3176
	20	Huamansaña	Huamansaña	0.91	718
	21	Huacapongo	Virú	5.68	908
	22	Quirihuac	Moche	8.44	1762
	23	El Tambo	Tambo	0.97	2183
Region V: Jequetepeque-Zarumilla	24	Yonán	Jequetepeque	32.69	3298
	25	Batan	Zaña	8.51	797
	26	Raca Rumi	Chancay-Lambayeque	38.49	2362
	27	Puente Ñacara	Piura	1.09	4495
	28	Puente Internacional Macara	Chira	1.99	1851
	29	Ciruelo	Chira	115.37	6979
	30	El Tigre	Tumbes	113.37	4663

2.2. Datasets

2.2.1. Surface Observations

Thirty hydrometric stations in the Pd (Table 1) were utilized, and their selection was based on the availability of data during the common data period of the SPP between 2007 and 2018 (12 years). This period contains a one-year warm-up period, as well as calibration and validation stages. Moreover, the selected hydrometric stations were typically located in the lower and middle parts of the basin, and their data were obtained from the official websites of the National Water Authority (ANA) and SENAMHI. These data were initially collected in m^3/s but were converted to mm/day for input into the model. The streamflow averages per station are presented in Table 1, and these flow rates vary according to their spatial location and the size of the basin.

2.2.2. Gridded Precipitation Products

The present study used three gridded precipitation products to evaluate their performance through streamflows simulations in the Pd. All of them were evaluated across the period of between 2007 and 2018 using the GR4J hydrological model. The first evaluated product is ERA5-Land reanalysis (top-down approach) from the European Centre for Medium-Range Weather Forecasts (ECMWF, Copernicus Climate Change service), as described by [31]. The other two SPP are derived from the bottom-up approach, namely SM2RAIN-ASCAT [11] and GPM + SM2RAIN [13].

ERA5-Land reanalysis provides hourly precipitation data accumulated at the daily time step. This product stands out for its global coverage in gridded format with a spatial resolution of 9 km. It is available from January 1950 to the present and can be accessed for free through its official webpage: https://cds.climate.copernicus.eu/cdsapp#!/dataset/reanalysis-era5-land?tab=overview (accessed on 12 March 2022).

The second precipitation product used is the SPP SM2RAIN-ASCAT, which provides daily precipitation data. This product follows a bottom-up methodology and has collected precipitation records since 2007. SM2RAIN-ASCAT has a spatial resolution of 12.5 km and is available in netCDF and raster formats. The development of this product is based on the inversion of the soil–water balance equation, allowing the estimation of the amount of water entering the soil. SM2RAIN-ASCAT was developed by [11], and different versions of the product can be found at the following link: https://zenodo.org/record/3635932#.YbfGn5FByUk (accessed on 20 March 2022).

The third product used is the SPP GPM + SM2RAIN. This product offers quasi-global precipitation data with a spatial resolution of 25 km. Similar to the previous product, GPM + SM2RAIN follows the bottom-up methodology and combines information from GPM's IMERG-LR product with precipitation estimates based on SM2RAIN derived from ASCAT H113 H-SAF, SMOS L3, and SMAP L3 soil moisture products [8,13]. This product is available from 2007 and can be downloaded for free in netCDF format from its official webpage: https://zenodo.org/record/3854817#.YbfHfJFByUk (accessed on 20 March 2022).

In addition to the use of these three precipitation products, the PISCO precipitation product [30], developed by SENAMHI, was also employed to generate daily streamflows in the 30 basins, and we used these streamflows as observed values when quantifying the Skill Score (SS). Moreover, SENAMHI's evapotranspiration product [32] was used to complement the input variables for the GR4J model.

Table 2 describes the main statistical characteristics of the daily precipitation time series. Consequently, it is observed that all three SPP recorded a minimum value of 0 mm. In terms of average values, ERA5-Land, SM2RAIN-ASCAT, and GPM + SM2RAIN averaged 4.48, 4.13, and 1.70 mm, respectively. Regarding the median values, ERA5-Land, SM2RAIN-ASCAT, and GPM + SM2RAIN obtained 2.99, 2.98, and 0.55 mm, respectively. As for the maximum values, ERA5-Land, SM2RAIN-ASCAT, and GPM + SM2RAIN reached 44.51, 24.18, and 21.36 mm, respectively. Given these descriptions, it is notable that the ERA5-Land values surpass the measurements of SM2RAIN-ASCAT and GPM + SM2RAIN, which could potentially have an impact on the generation of daily streamflows.

Table 2. The main statistical characteristics of the SPP, SM2RAIN-ASCAT (A), GPM + SM2RAIN (G), and ERA5-Land (E).

Region (AAA)	ID	Minimun			Mean			Median			Maximun		
		(A)	(G)	(E)	(A)	(G)	(E)	(A)	(G)	(E)	(A)	(G)	(E)
Region I: Caplina-Ocoña	1	0.0	0.0	0.0	2.1	0.6	1.8	0.5	0.0	0.1	20.5	22.0	34.6
	2	0.0	0.0	0.0	2.1	0.4	2.2	0.5	0.0	0.4	20.5	13.7	23.3
	3	0.0	0.0	0.0	1.7	1.1	2.6	0.6	0.1	1.0	10.3	11.6	23.6
	4	0.0	0.0	0.0	2.0	1.2	2.4	1.1	0.2	0.8	9.9	11.3	33.3
	5	0.0	0.0	0.0	2.7	1.6	3.0	1.3	0.4	1.5	17.0	11.6	23.8
Region II: Chaparra-Chincha	6	0.0	0.0	0.0	4.7	1.1	3.9	4.0	0.2	2.4	18.1	11.7	28.6
	7	0.0	0.0	0.0	2.9	0.9	4.2	1.0	0.0	3.1	23.6	19.1	29.4
Region III: Cañete-Fortaleza	8	0.0	0.0	0.0	3.7	1.8	4.5	2.6	0.6	3.3	16.9	17.5	29.7
	9	0.0	0.0	0.0	3.5	1.8	4.6	2.7	0.8	3.9	13.5	28.1	43.4
	10	0.0	0.0	0.0	3.3	1.3	4.8	2.5	0.3	4.0	12.9	13.0	46.6
	11	0.0	0.0	0.0	4.2	0.9	5.5	3.3	0.1	4.8	17.2	13.0	29.6
	12	0.0	0.0	0.0	3.9	1.9	5.1	3.8	0.5	4.2	18.2	26.7	25.6
	13	0.0	0.0	0.0	4.4	1.4	5.3	4.0	0.5	3.7	21.2	13.4	65.9
	14	0.0	0.0	0.0	3.9	2.2	4.0	4.0	0.9	3.0	17.1	22.7	33.9
	15	0.0	0.0	0.0	5.1	1.7	5.6	4.4	0.7	4.4	24.0	24.0	26.9
	16	0.0	0.0	0.0	2.2	0.5	2.5	1.2	0.0	1.2	14.9	9.0	22.1
	17	0.0	0.0	0.0	4.7	2.6	5.1	4.4	1.9	4.0	16.7	18.1	28.4
	18	0.0	0.0	0.0	4.3	1.1	4.9	2.9	0.4	3.7	20.5	9.6	26.8

Table 2. *Cont.*

Region (AAA)	ID	Minimun			Mean			Median			Maximun		
		(A)	(G)	(E)	(A)	(G)	(E)	(A)	(G)	(E)	(A)	(G)	(E)
Region IV: Huarmey-Chicama	19	0.0	0.0	0.0	5.5	2.1	5.9	4.9	1.0	4.7	26.0	14.0	36.1
	20	0.0	0.0	0.0	3.9	1.0	4.0	2.8	0.2	2.7	27.5	15.0	37.7
	21	0.0	0.0	0.0	5.0	1.4	4.8	4.0	0.5	3.6	33.3	20.5	34.4
	22	0.0	0.0	0.0	4.1	1.4	4.2	3.0	0.4	3.1	24.4	20.6	34.5
	23	0.0	0.0	0.0	5.3	2.1	6.1	4.0	0.8	4.3	30.9	22.8	40.9
Region V: Jequetepeque-Zarumilla	24	0.0	0.0	0.0	6.7	2.2	5.8	5.4	0.8	3.9	31.2	28.1	56.3
	25	0.0	0.0	0.0	5.3	1.6	3.2	3.7	0.0	0.9	29.2	21.5	48.5
	26	0.0	0.0	0.0	5.0	2.5	4.5	4.1	0.9	3.4	25.1	28.8	35.3
	27	0.0	0.0	0.0	4.2	1.8	5.2	1.7	0.4	3.4	66.8	41.4	110.9
	28	0.0	0.0	0.0	5.5	4.0	5.5	2.8	1.6	2.3	45.8	47.2	138.3
	29	0.0	0.0	0.0	5.2	3.7	6.0	3.3	1.4	3.3	33.5	42.9	90.2
	30	0.0	0.0	0.0	6.7	3.2	7.3	4.8	0.8	4.7	38.6	41.9	96.6

3. Methods

The development of this research was divided into three main stages: (1) Hydrological modeling with GR4J; (2) Performance evaluation of the 3 precipitation products using efficiency metrics; (3) Evaluation of the streamflow time series using Skill Score and hydrological signatures (Figure 2).

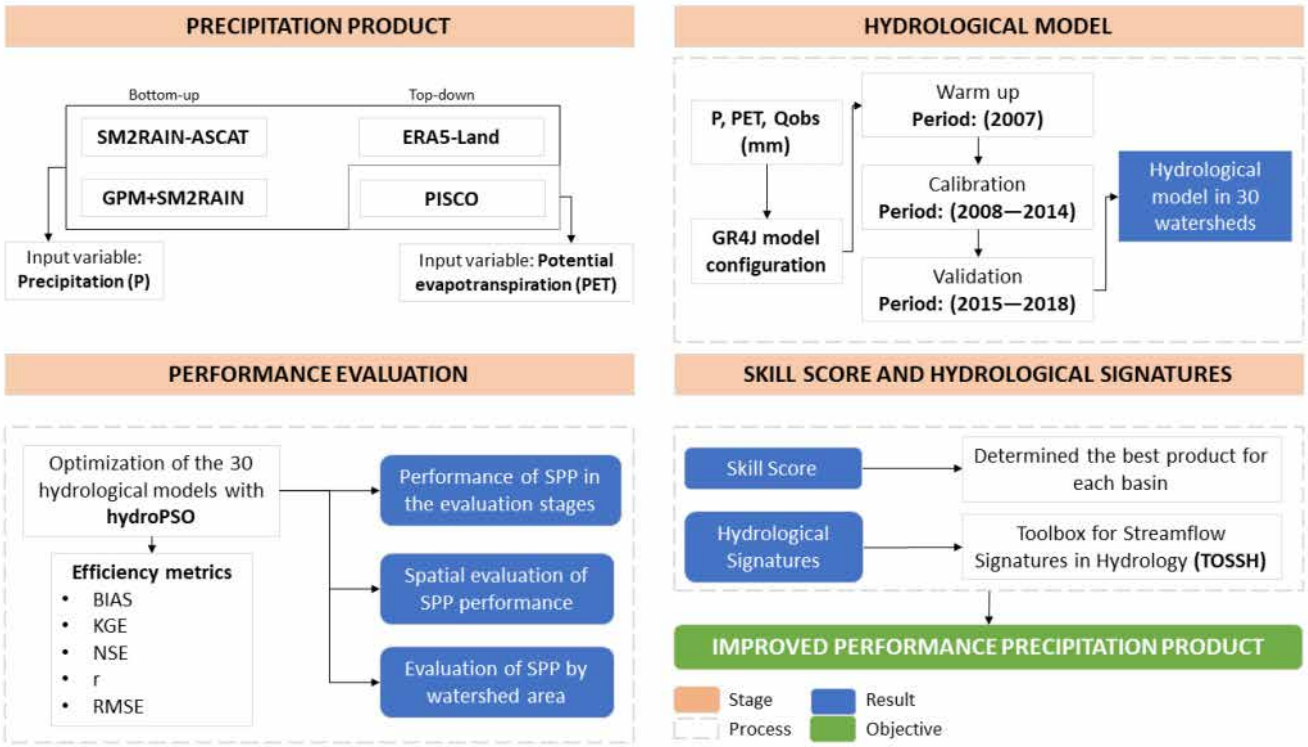

Figure 2. Methodological diagram for the evaluation of precipitation products for streamflow generation in the Pd.

3.1. Hydrological Modeling

The model required precipitation, evapotranspiration, and streamflow data from the hydrometric stations as input for the calibration and validation procedures. The airGR package, coded in the R programming language, was used for model execution, and is freely available for use https://github.com/cran/airGR (accessed on 14 June 2022).

The rainfall-runoff model used in this study is the Génie Rural à 4 paramètres Journalier (GR4J) [33]. This conceptual model is a deterministic and lumped model with four parameters updated at daily time step. To operate, the model requires daily precipita-

tion and evapotranspiration data, as well as a series of observed streamflow data for the calibration and validation process.

The GR4J model Is composed of two reservoirs. The first reservoir, referred to as "S", relates evapotranspiration and precipitation to determine the precipitation volume. The second reservoir, referred to as "R", represents the infiltration processes within the basin. The GR4J model is widely used in hydrological studies due to its ability to simulate streamflow behavior in basins. Its structure and parameters allow for an adequate representation of key hydrological processes, making it a valuable tool for hydrological modeling and water resource management [34,35].

The model consists of four parameters, which are adjusted during the calibration process for each case study. Additionally, two initial values, R and S, are required to initiate the simulation. The necessary initial values are described in Table 3, while Table 4 specifies the model parameters and recommends initial values.

Table 3. Initial values in the GR4J hydrological model [33].

Parameter	Unit	Description
R	m	Initial water level in the first reservoir
S	m	High of the second reservoir

Table 4. Parameters of the GR4J hydrological model [33].

Parameter	Unit	Description	Initial Value
X1	m	First reservoir capacity	5.9
X2	m	Water interchange coefficient	0.0
X3	m	Second reservoir capacity	4.5
X4	dt	Base time of the unit hydrograph	0.2

The GR4J model has been successfully applied in various basins, in countries all around the world, including Peru [35], and it has been widely accepted due to its parsimony in hydrology. In this study, the GR4J model was used to generate daily streamflows in 30 basins located in the Pd. The precipitation and evapotranspiration data described in the section were used as input data for the model.

3.2. Performance Evaluation of the 3 Precipitation Products

As expected, a calibration and validation process were necessary to evaluate the model outputs and, consequently, assess the performance of the three precipitation products. The metrics used are detailed in Table 5, and the calibration and validation process were performed using the hydroPSO package [36], which is described on its official page https://github.com/hzambran/hydroPSO (accessed on 21 August 2022). hydroPSO has been deemed suitable for countless hydrological models, providing satisfactory analysis [37–41]. In the application of a hydrological model, it is essential to assess the agreement between the simulated and observed streamflows. In this study, this evaluation was carried out using five efficiency metrics for the calibration, validation, and overall periods. The efficiency metrics used are the Nash-Sutcliffe Efficiency (NSE), Kling-Gupta Efficiency (KGE), Root Mean Square Error (RMSE), Relative Bias (BIAS), and the Pearson Correlation coefficient (r). These indicators are widely used in the scientific literature and have been applied in numerous research studies [42]. Specific details about the efficiency metrics can be found in Table 5. Additionally, authors such as [43] have successfully employed these statistical indicators.

Table 5. Statistical efficiency indicators [44].

Statistics	Equation	Ideal Value
Nash Sutcliffe Efficiency	$NSE = 1 - \frac{\sum_{i=1}^{n}\left(Q_{simi} - Q_{refi}\right)^2}{\sum_{i=1}^{n}\left(Q_{refi} - Q_{ref}\right)^2}$	1
Kling Gupta Efficiency	$KGE = 1 - \sqrt{\left(\frac{Qsim}{Qobs}\right)^2 + \left(\frac{1}{Bias}\right)^2 + (r-1)^2}$	1
Root Mean Square Error	$RMSE = \sqrt{\frac{\sum_{i=1}^{n}(P_{obsi} - P_{simi})^2}{n}}$	0
Relative Bias	$BIAS = \frac{1}{n}\sum_{i=1}^{n}\left(\frac{P_{simi} - P_{obsi}}{P_{obsi}}\right)$	0
Pearson Correlation coefficient	$r = \frac{n(\sum_{i=1}^{n} P_{simi}P_{obsi}) - (\sum_{i=1}^{n} P_{simi})(\sum_{i=1}^{n} P_{obsi})}{\sqrt{\left[n\sum_{i=1}^{n} P_{simi}^2 - (\sum_{i=1}^{n} P_{simi})^2\right]\left[n\sum_{i=1}^{n} P_{obsi}^2 - (\sum_{i=1}^{n} P_{obsi})^2\right]}}$	1

In addition, efficiency intervals were used to classify the obtained results when comparing the simulated and observed streamflow time series. These intervals provide a classification of the model performance based on the level of agreement between the simulated and observed values. They allow for a qualitative assessment of the model's ability to reproduce the observed streamflow patterns [45] (Table 6).

Table 6. Referential values for efficiency metrics [45].

Performance Rating	NSE	BIAS
Very Good	0.75–1.00	$\leq \pm 10$
Good	0.65–0.75	± 10–± 15
Satisfactory	0.50–0.65	± 15–± 25
Unsatisfactory	<0.50	$\geq \pm 25$

3.3. Evaluation of the Series Using Skill Score and Hydrological Signatures

The use of the Skill Score allowed us to compare daily simulated streamflows from precipitation products using a reference streamflow. It determined the best product for each basin and, consequently, helped to select the best product for each region [18]. Additionally, to find the 10 hydrological signatures described in Table 7, a code developed in MATLAB, called the Toolbox for Streamflow Signatures in Hydrology (TOSSH) [46] https://github.com/TOSSHtoolbox/TOSSH (accessed on 10 October 2022), was used.

Table 7. Hydrological signatures considered in this study [18].

Attribute	Long Name	Unit
Mean Q	Mean daily streamflow	$mm.day^{-1}$
Q5	Streamflow 5th quantile	$mm.day^{-1}$
Q95	Streamflow 95th quantile	$mm.day^{-1}$
Q7-day min	7-day minimum streamflow	-
High Q frequency	Max streamflow frequency	y^{-1}
High Q duration	Max streamflow duration Min streamflow frequency	days
Low Q frequency	Min streamflow duration	y^{-1}
Low Q duration	Mean daily streamflow	days
BFI	Baseflow index	-
FDC slope	The slope of the flow duration curve	-

3.3.1. Skill Score

The Skill Score (SS) efficiency metric was implemented to evaluate the goodness-of-fit of each precipitation product (Equation (1)). This approach was adopted to account for the inherent variability of the basin under adverse streamflow generation conditions [18]. Therefore, simulated streamflows from the precipitation products were compared with the

streamflow simulated using the PISCO precipitation product. The reference for the use of the Skill Score can be found in the work of [47].

$$SS = 1 - \frac{\sum_{i=1}^{n}(Q_{simS} - u_{obs})^2}{\sum_{i=1}^{n}(Q_{simG} - u_{obs})^2} \quad (1)$$

3.3.2. Hydrological Signatures

The estimation of hydrological characteristics, known as streamflow signatures or hydrological signatures, aims to obtain a comprehensive understanding of basin behavior and evaluate the long-term reliability of precipitation products. These hydrological signatures quantify aspects related to the magnitude, frequency, duration, timing, and rate of change of hydrological events. In this study, the Toolbox for Streamflow Signatures in Hydrology (TOSSH) developed by [46] was used to calculate the hydrological signatures. This approach allowed the variability characterization of the 30 streamflow time series and the analysis of specific hydrological phenomena, such as high or low flows. The calculation and analysis of these 10 hydrological signatures (Table 7) provided key information about the basin's behavior, enabling a better understanding of its hydrological response.

4. Results

The evaluation of the three Satellite Precipitation Products (SPP) revealed a range of outcomes across the entire extent of the Pacific drainage (Pd). These results underwent analysis using efficiency metrics such as the Kling-Gupta Efficiency Coefficient (KGE), Nash-Sutcliffe Coefficient (NSE), correlation coefficient (r), and bias (BIAS). Additionally, it was observed that these results also exhibited variations depending on the analysis region and were possibly influenced by factors like the basin size and climate or morphological characteristics.

4.1. Performance of Satellite Products in the Evaluation Stages

The comparative analysis among the calibration, validation, and total periods reveals that, in general, all three products demonstrated reliability at various stages of the analysis (Figure 3). During the calibration period, the most closely fitting efficiency metrics were achieved and, as expected, these values decreased during the validation and the overall period.

The assessment of the three analysis periods was conducted by comparing the NSE, KGE, BIAS, and RMSE metrics between the extreme and average values of the three Satellite Precipitation Products (SPP) and was visualized through boxplots.

When considering the NSE efficiency metric for the ERA5-Land product and evaluating the average values, satisfactory results were observed during the calibration period (>0.65), acceptable results in the overall period (>0.50), and unsatisfactory results during the validation period (<0.50). GPM + SM2RAIN presents the same results as those obtained with ERA5-Land.

On the other hand, the SM2RAIN-ASCAT product exhibited an outstanding performance across all three periods, achieving good results during the calibration period (>0.65), satisfactory results in the overall period (>0.50), and satisfactory results during the validation period (>0.50). Considering the KGE efficiency for the ERA5-Land product and evaluating the average values, very good results were obtained during the calibration period (>0.75), good results in the overall period (>0.65), and satisfactory results during the validation period (>0.50). GPM + SM2RAIN presents the same results as those obtained with ERA5-Land.

In contrast, the SM2RAIN-ASCAT product demonstrated an outstanding performance in all three periods, achieving very good results during the calibration period (>0.75), satisfactory results in the overall period (>0.50), and again satisfactory results during the validation period (>0.50).

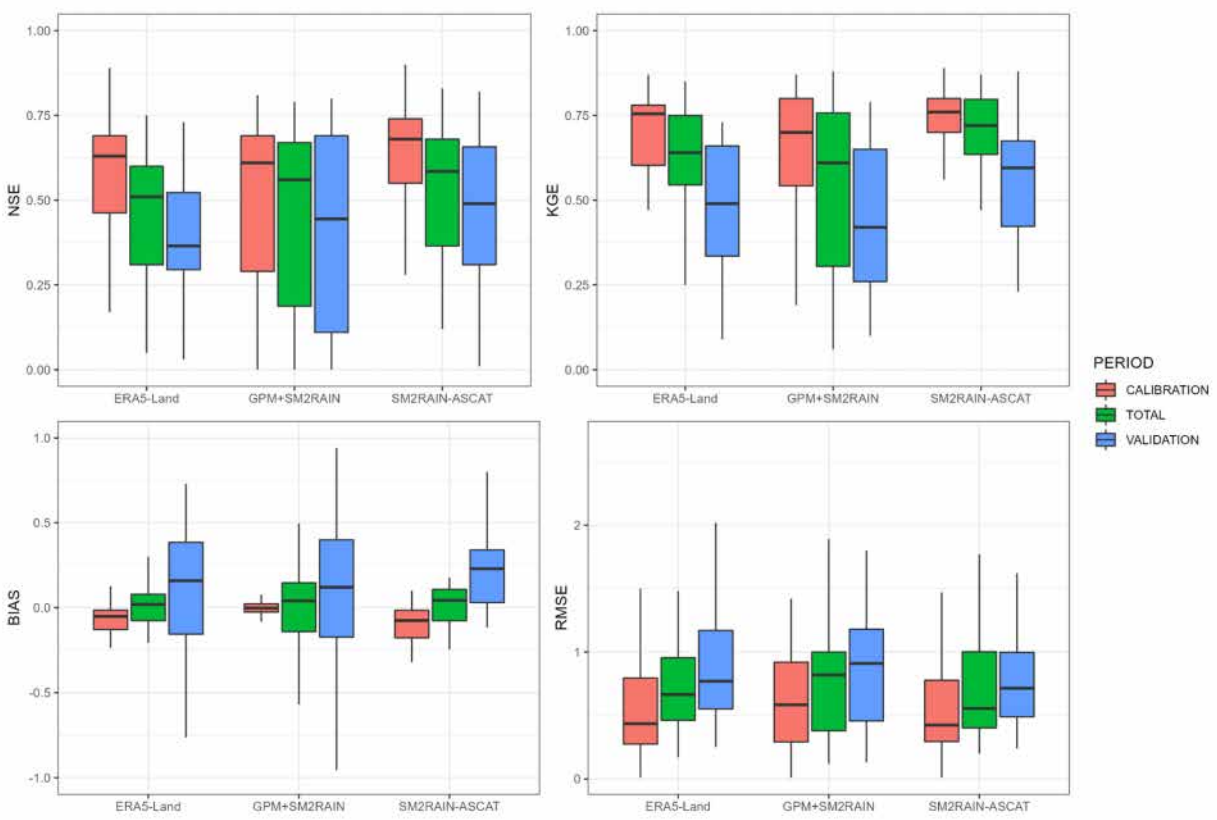

Figure 3. Boxplot comparing efficiency metrics (NSE, KGE, BIAS and RMSE) between the calibration, validation, and total period phases of the hydrological modeling.

Regarding the BIAS efficiency metric in the three evaluated products, it was determined that the GPM + SM2RAIN product had the mean closest to 0 in the calibration, validation, and total periods. However, it also exhibited greater variation in underestimation and overestimation. In the RMSE metric, the mean values of the products approach 0.5, and the SM2RAIN-ASCAT product shows a more stable root mean square error across all three analysis phases.

Based on the evaluation conducted in the 30 basins, it can be concluded that the evaluated products showed promising results. All three products mostly yielded results in the range of >0.50 for the calibration stage in the NSE and KGE metrics. Most of the RMSE and BIAS results were close to 0, indicating a good performance. Additionally, the r metric showed the highest number of basins in the range of 0.65.

4.2. Evaluation of the Performance of Precipitation Products in the Pd

The performance, considering the spatial variability of the three Satellite Precipitation Products (SPP) in the estimation of daily mean streamflows during the calibration period, is presented in Figures 4 and 5. These figures provide details regarding the local performance in different regions within the study area.

In Figure 4a, the distribution of BIAS is presented. According to Moriasi [45], this metric is considered highly satisfactory within the range of −0.10 to +10, while it is deemed unsatisfactory if the variation falls below −0.25 or above +0.25. In this representation, red color shades indicate significant underestimations, blue shades indicate marked overestimations, and white values highlight optimal results. For ERA5-Land, the most favorable results are observed in region V, while region I shows a less satisfactory performance. On the other hand, the GPM + SM2RAIN product exhibits an outstanding performance along the Pacific drainage, with all basins in region III yielding results within the range of −0.10 to +0.10.

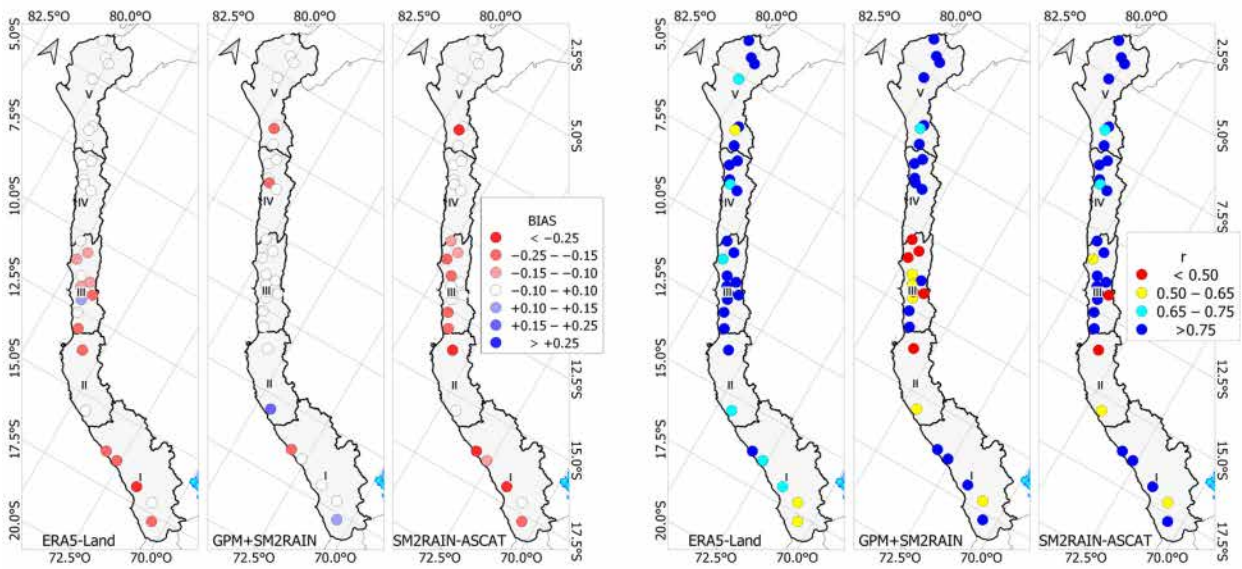

(**a**) (**b**)

Figure 4. Distribution of the efficiency metrics of the 30 basins in the calibration phase. (**a**) BIAS; (**b**) r.

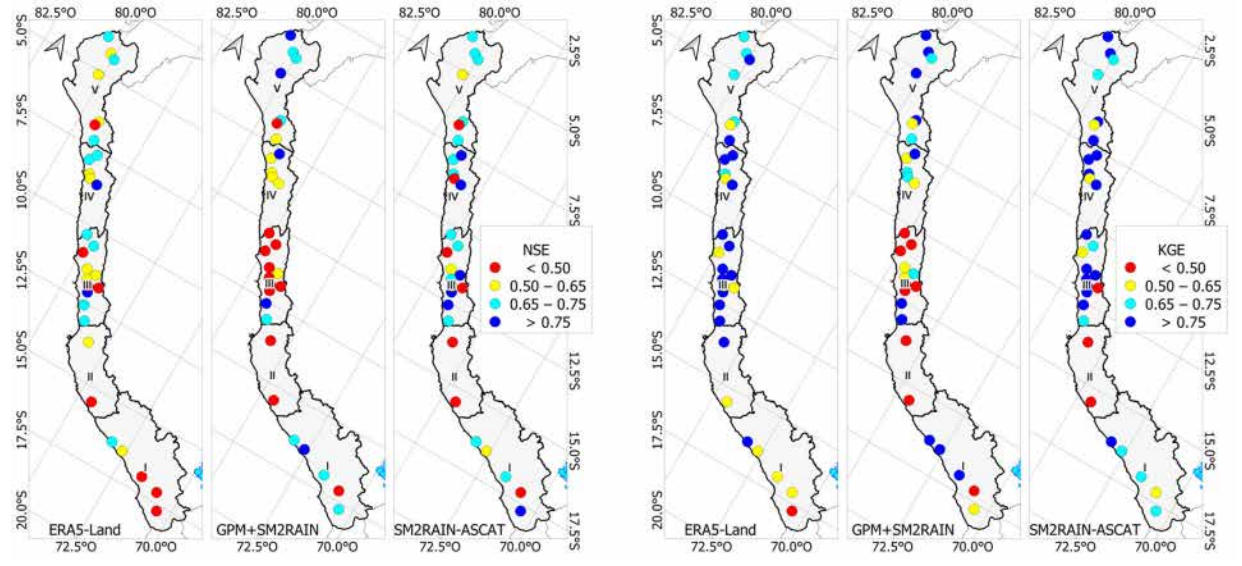

(**a**) (**b**)

Figure 5. Distribution of the efficiency metrics of the 30 basins in the calibration phase. (**a**) NSE; (**b**) KGE.

Figure 4b provides an analysis of the Pearson correlation coefficient results for the study area. In this representation, red shades indicate unsatisfactory results, while blue shades reflect a high degree of agreement. For ERA5-Land, the results show satisfactory levels ($r > 0.5$) in all 30 basins, with an exceptional performance in regions II, III, and IV. However, the lowest metric is observed only in region I. In contrast, the GPM + SM2RAIN product stands out for its performance in regions I, IV, and V, although it presents unsatisfactory results in region II and the northern part of region III.

For SM2RAIN-ASCAT, very encouraging results were obtained with Pearson correlation coefficients exceeding 0.75 in regions I, III, IV, and V. However, region II was the only one predominantly exhibiting an unsatisfactory correlation coefficient, with values below 0.5. These findings complete the comprehensive evaluation of the performance of the analyzed products in the hydrological study.

Figure 5 presents the results derived from the NSE and KGE metrics, using a color scale to indicate different levels of performance. The blue shade represents an outstanding performance (>0.75), cyan denotes a good performance (>0.65), yellow reflects a satisfactory performance (>0.50), and red indicates an unsatisfactory performance (<0.50).

In Figure 5a, the point distribution of the NSE results in the study area is displayed. In this context, ERA5-Land shows the best results in region IV, while region I has the highest concentration of basins with an unsatisfactory performance. On the other hand, the GPM + SM2RAIN product stands out in regions I and V, predominantly showing satisfactory results, in contrast to region II and the northern part of region III, where more basins exhibit an unsatisfactory performance. Regarding SM2RAIN-ASCAT, it demonstrates a very positive performance in regions I, III, and IV, while region II predominantly registers unsatisfactory results.

Similarly, Figure 5b presents the results of the KGE metric, which uses the same color scale as NSE, but with higher scores. ERA5-Land exhibits outstanding results in 29 of the 30 evaluated basins, particularly in regions III and IV, with lower scores observed only in region I. GPM + SM2RAIN excels in regions IV and V but shows unsatisfactory results in the northern part of region III and region II. As for SM2RAIN-ASCAT, it stands out with very favorable results, especially in regions III, IV, and V, while region II exhibits unsatisfactory results (KGE < 0.50).

The precipitation product results exhibited variations in the different study areas, where the bottom-up approach demonstrated efficiency throughout the study area, often surpassing the performance of ERA5-Land. Figure 6 presents the results for five selected hydrographic basins for each region, highlighting that the best results were obtained in the northern (IV, V) and southern (I) regions, while the central region (III) exhibited greater variability in the results. Additionally, region II yielded fewer promising results for the SM2RAIN-ASCAT and GPM + SM2RAIN products, with only the ERA5-Land product providing efficient metrics.

Furthermore, in Figure 6, the calibration and validation periods are displayed, revealing a decrease in efficiency during the validation period. The streamflows generated from the Satellite Precipitation Products (SPP) generally matched the observed records. However, in specific cases, such as in regions II and III, ASCAT-SM2RAIN and GPM + SM2RAIN struggled to match during low-flow periods. It is also observed that in some basins, the flow records had gaps, as shown in Figure 6b, where the absence of flow data is evident for the years 2011–2013.

Figure 6 also illustrates the monthly hydrological regime of the observed flow and the time series of simulated flow derived from the precipitation products. This analysis of the hydrological regime demonstrates the similarity between the simulated and observed flows during high-flow and low-flow periods. For example, this similarity is particularly noticeable in regions II, III, and V. In contrast, in region IV, there is a clear overestimation during low-flow months by ASCAT-SM2RAIN and GPM + SM2RAIN. Additionally, Figure 6 also shows the variation in flow according to the chosen region, and this variation is influenced by the spatial location (increased flow from south to north). However, these differences in flows are also due to the extent of the studied basin.

4.3. Spatial Performance Evaluation by Areas of the Precipitation Products

From the previous analysis, it clearly shows that the basins demonstrate a robust hydrological response over the study period (with the Pd efficiency metrics ranging between 0.5 and 0.75). However, it is also clear that the evaluated basins vary in terms of size in square kilometers (km^2), which could influence the flow response. Figure 7 displays histograms organized according to the results of the Kling-Gupta Efficiency Coefficient (KGE) and segmented into ranges based on the Moriasi classification (Unsatisfactory < 0.5; Satisfactory 0.50–0.65; Good 0.65–0.75; and Very Good 0.75–1.00). In addition to the range segmentation, the 30 basins were distributed into 4 categories: basins less than 1000 km^2, 1000 to 2500 km^2, 2500 to 5000 km^2, and over 5000 km^2.

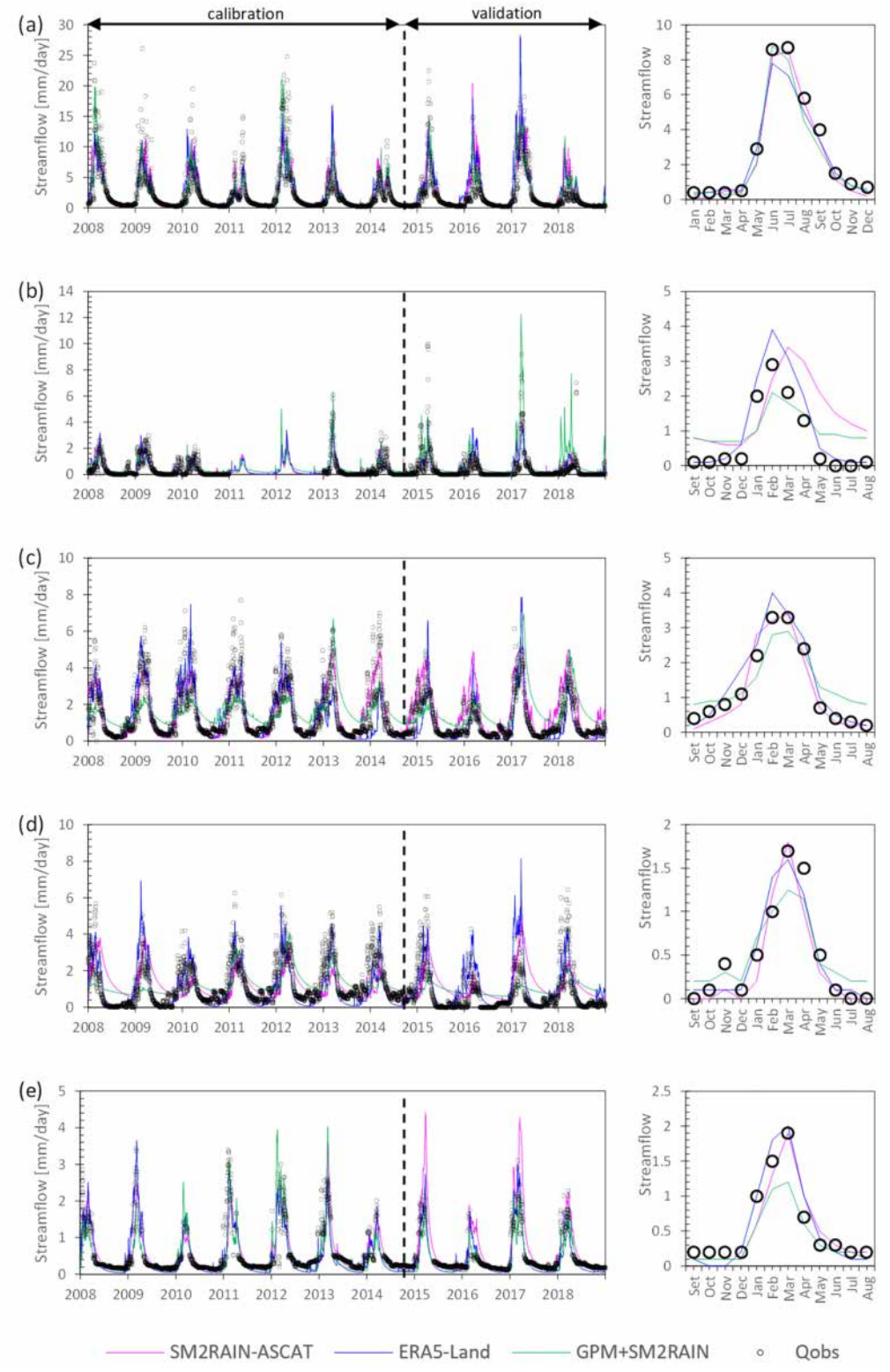

Figure 6. Simulated daily streamflow during the calibration and validation stages by GR4J using the precipitation products SM2RAIN-ASCAT (purple line), ERA5-Land (blue line), and GPM + SM2RAIN (green line). The black dots represent the observed discharge. (**a**) Region V: El Tigre; (**b**) Region IV: Quirihuac; (**c**) Region III: Obrajillo; (**d**) Region II: Letrayoc; (**e**) Region I: Ocoña.

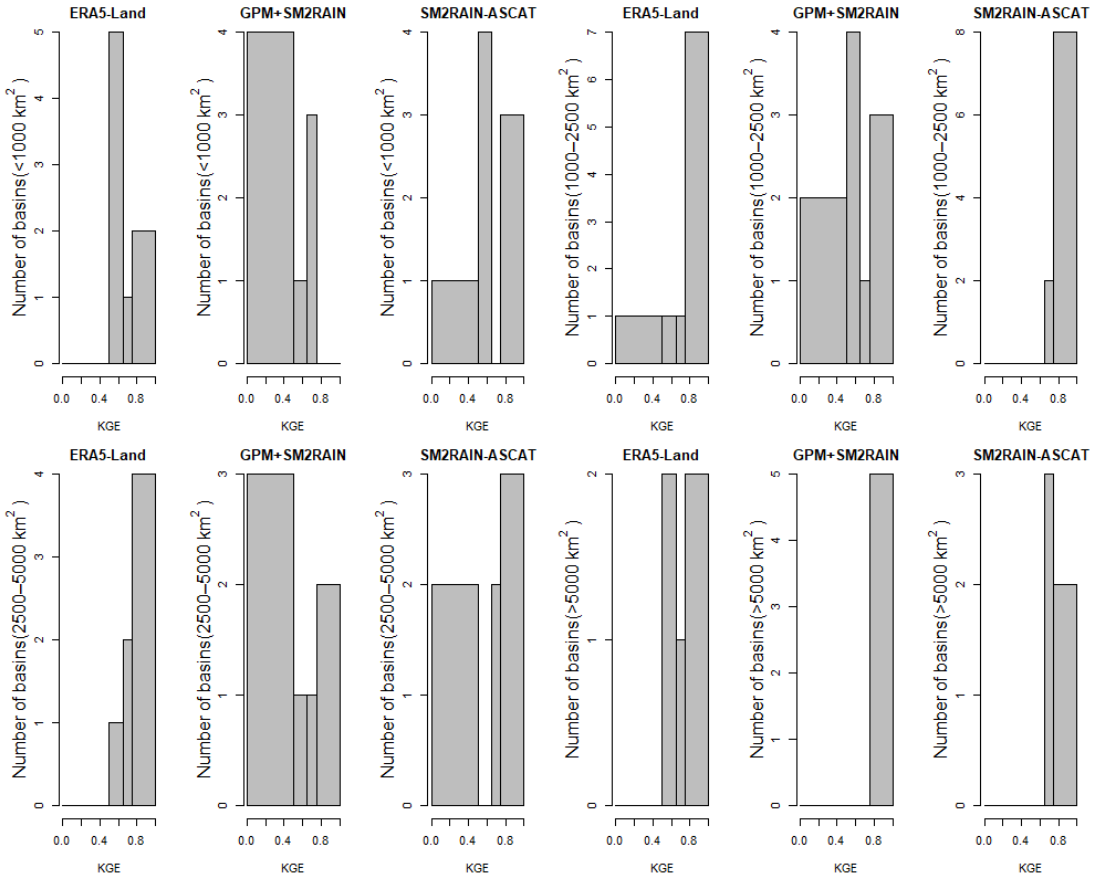

Figure 7. Performance scores for the KGE metric (X-axis) during the calibration stage. The histograms represent the performance of the precipitation products in relation to the size of the analyzed basins (Y-axis).

In basins of an area smaller than 1000 km^2 (8 basins), ERA5-Land achieved a KGE greater than 0.5 (Satisfactory) in all eight basins, primarily excelling, with five basins rated as Satisfactory and the remaining three with Good and Very Good ratings. In contrast, GPM + SM2RAIN achieved a KGE greater than 0.5 in four out of the eight basins, resulting in one basin with a Satisfactory rating and three with Good ratings. For SM2RAIN-ASCAT, a KGE greater than 0.5 was recorded in seven out of the eight basins, resulting in four Satisfactory and three Very Good ratings. Subsequently, for basins with areas between 1000 and 2500 km^2 (10 basins), ERA5-Land achieved a KGE greater than 0.5 in nine out of the ten basins, with seven basins demonstrating Very Good performance. GPM + SM2RAIN, on the other hand, achieved a KGE greater than 0.5 in eight out of the ten basins, with Satisfactory (4), Good (1), and Very Good (3) results. Similarly, SM2RAIN-ASCAT surpassed the threshold of 0.5 in all ten basins, standing out with eight basins in the Very Good category (>0.75).

In the basins with areas between 2500 and 5000 km^2 (7 basins), ERA5-Land obtained a KGE greater than 0.5 in all seven basins, with a remarkable performance in four basins in the Very Good category. GPM + SM2RAIN exceeded the value of 0.5 in four out of the seven basins, resulting in Satisfactory (1), Good (1), and Very Good (2) ratings. SM2RAIN-ASCAT achieved results above Satisfactory in five out of the seven basins, with ratings of Good (2) and Very Good (3). Finally, for basins larger than 5000 km^2 (5 basins), all three SPP presented results above Satisfactory. Among them, GPM + SM2RAIN demonstrated the highest number of Very Good results (5 basins), followed by SM2RAIN-ASCAT with Good (3) and Very Good (2) ratings, while ERA5-Land had two Satisfactory basins, one Good basin, and two Very Good basins.

4.4. Improved Performance

The quantification of the efficiency metrics NSE, KGE, RMSE, r, and BIAS showed a satisfactory performance of the precipitation products in generating simulated daily streamflows. However, this study aims to determine the best product for each hydrographic basin and the region defined by the AAA. Therefore, the Skill Score (SS) index was used, which involved comparing the simulated flows from the three products with a reference streamflow. Although 30 hydrometric stations were used for the calibration and validation stage, these records had missing data for multiple years. Thus, they could not be used to quantify the Skill Score, as this metric requires a complete time series. In this context, the streamflows generated by PISCO in each of the basins were used as the reference flow for comparison. The results are shown in Figure 8. Among the 30 analyzed basins, ERA5-Land, GPM + SM2RAIN, and SM2RAIN-ASCAT were predominant in 5, 12, and 13 basins, respectively. Additionally, in the northern zone of region 5, there is a predominance of the GPM + SM2RAIN product. In region 4, the SM2RAIN-ASCAT and GPM + SM2RAIN products showed predominance in 2 basins each. In region 3, SM2RAIN-ASCAT predominated in the northern part, while GPM + SM2RAIN predominated in the southern part. In region 2, ERA5-Land predominated, and finally, in region 1, GPM + SM2RAIN predominated.

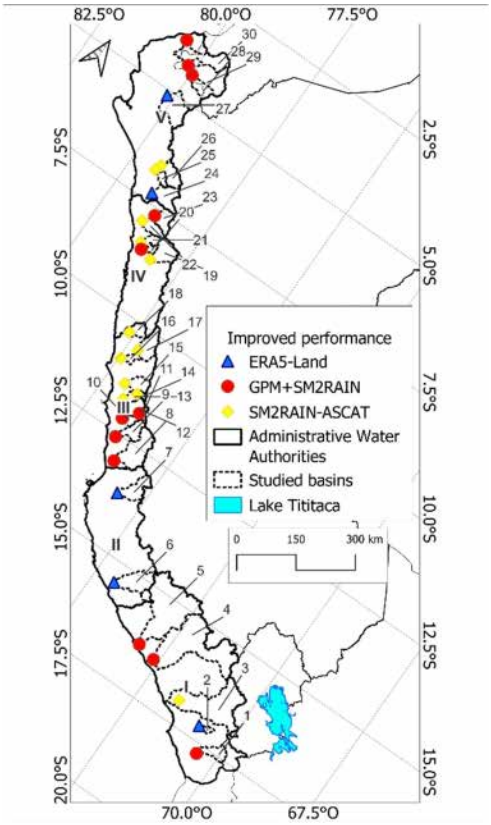

Figure 8. Results of the Skill Score (SS) for the SM2RAIN-ASCAT, ERA5-Land, and GPM + SM2RAIN SPP compared to the simulated flows by PISCO, indicating the best product in each analyzed basin.

4.5. Reliability of Remote Sensing Products on Hydrologic Signatures

The variability of the simulated streamflows was quantified using hydrological signatures, where it is worth noting that the signatures with the best performance were Mean Q, Q95, Q5, and Q7, respectively, as they consistently obtained values above 0.80 on average. On the other hand, the BFI and DL signatures had average values below 0.5. Figure 9 provides quantitative (left) and qualitative (right) analysis to identify the performance of each product with respect to the hydrological signature. It is also important to note that the

performance of the precipitation product and the hydrological model is not uniform across all basins, which could be attributed to the characteristics of the precipitation products or the functioning scheme of the hydrological model. In region I, the product that showed the best response was GPM + SM2RAIN, with Mean Q being the best-represented signature and Low Frequency being the worst-represented. In region II, GPM + SM2RAIN showed the best response, with Minimum 7-day Flow as the best-represented signature and High Duration as the worst-represented. In region III, the product that showed the best response was GPM + SM2RAIN, with Low Frequency being the best-represented signature and High Duration being the worst-represented. In region IV, SM2RAIN-ASCAT showed the best response, with Minimum 7-day Flow as the best-represented signature and Base Flow Index as the worst-represented. In region V, SM2RAIN-ASCAT showed the best response. Q95 was the best-represented signature and Long Duration was the worst-represented. Thus, the evaluation of the precipitation products' performance using hydrological signatures allowed for the identification of the best representations of maximum, minimum, and base flow streamflows, highlighting that these products better represent average streamflows.

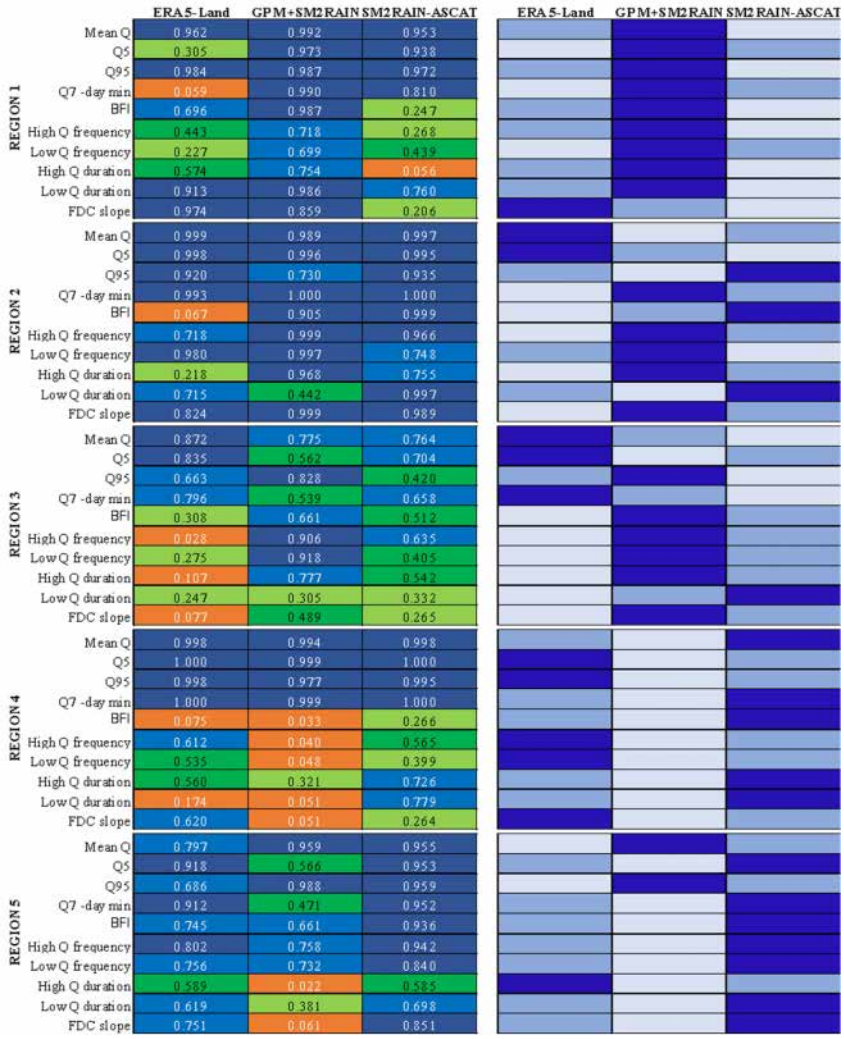

Figure 9. Hydrological signatures of the simulated streamflows by GR4J (ERA5-Land, GPM + SM2RAIN, and SM2RAIN-ASCAT, read from left to right). The left panel represents the capability of the precipitation product to represent each hydrological signature in terms of the correlation coefficient. where dark blue shows best performance, green shows medium performance, and orange shows low performance. The right panel represents the capability to represent the hydrological signature in each region, where dark blue indicates the best performance and light blue the worst performance.

5. Discussions

5.1. Intrinsic Quality of Satellite Precipitation Products

The evaluation conducted on gridded products using a bottom-up approach allowed us to comprehend and interpret the performance of each product along the Pacific drainage and establish connections between the results and the climatic and physiographic characteristics of the basins. The performance was validated against the observed records using efficiency metrics such as NSE, KGE, RMSE, BIAS, and r.

Products like SM2RAIN-ASCAT and GPM + SM2RAIN have demonstrated satisfactory outcomes in their application in basins worldwide [24,48], occasionally surpassing other satellite-based precipitation products (SPP). Nevertheless, the effectiveness of soil moisture-based products also depends on the topographical, climatic, and other specific conditions of the basin, and in some cases, they may be outperformed by other SPP [49].

For instance, SM2RAIN-ASCAT and SM2RAIN-CCI products exhibit higher accuracy in arid areas such as the Peruvian and Bolivian Altiplano region than in the southern Asia region in Pakistan [14]. This precision is also confirmed in our study area. This disparity can be attributed to the more favorable physical environment for satellite-based soil moisture (SM) estimations in the Altiplano region.

Furthermore [15], various SPP were compared in a mountainous basin with a humid subtropical monsoonal climate in southern China and it was found that other SPP adapted better than bottom-up-focused SPP to the basin's climatology. This could be mainly attributed to the steep slopes in the mountainous basin and the predominant climate due to the geographical location. Likewise, in this study, the results varied depending on the rainfall climatology, received precipitation, and basin size. As demonstrated by [50] in Pakistan, basins with precipitation exceeding 700 mm did not yield encouraging results, whereas basins with precipitation below 100 mm (arid and hyper-arid zones) exhibited Very Good adjustments, as observed in the results presented in this research. It should be noted that precipitation is generally directly proportional to altitude, which implies that basins predominantly featuring flat areas may yield better results, as demonstrated by various authors [51–53].

Prominent discrepancies and sources of uncertainty in these areas arise from the impact of complex topography and climatic variability, phenomena extensively documented in previous research [23,54]. Thus, the results of this investigation demonstrated that the efficiency of SPP is also related to the slope and extent of the basin. Small, steep basins like Supe encountered difficulties in replicating the observed streamflows, while, conversely, large, low-gradient basins like Camaná displayed Very Good results (NSE > 0.75).

It is anticipated that the most significant positive or negative biases will manifest in SM2RAIN-based products in forested areas with dense vegetation cover (such as glaciers and mountainous regions in wet regions), where satellite sensors may be interpreted as being unable to penetrate dense vegetation [55], or in regions where the soil remains saturated for prolonged periods, such as inundated areas (specifically in hydraulically developed areas in wet regions) [56].

5.2. Performance of Hydrological Modeling on the Pd

The Pacific drainage (Pd) is an important region, making it crucial to adapt new methodologies related to water resource availability, such as the assessment of Underexplored Satellite Precipitation Products (SPP) in South America. In this context, selecting an appropriate hydrological model is a significant task. In this study, similar to other studies [57], the GR4J model was chosen. This model was selected because it has demonstrated satisfactory results (NSE > 0.5) in several basins in Peru [34,58].

While the GR4J model showed very promising results in this research, it is worth noting that some basins obtained unsatisfactory metrics for all three SPP, as observed at the Yauca hydrometric station. These modeling uncertainties could be attributed to basins like Yauca having insufficient streamflow records (3 years), which hindered the calibration process. Unlike other semi-distributed or distributed models, like SWAT, TOPMODEL, and

TOPKAPI, the GR4J model is a lumped model with four parameters and two functioning tanks, which may be inadequate for basins with diverse climates and complex topographies. Additionally, it should be noted that in basins with significant human intervention, such as the Rimac basin, the adaptation of the GR4J model can be further complicated as streamflows may not be naturalized.

Despite experiencing a variety of climates, the Pacific drainage (Pd) showed that GR4J could produce satisfactory results, even in arid climates [50]. Furthermore, the evaluation of SPP and the GR4J model also encompassed basins of different sizes in square kilometers (km^2), demonstrating that the best results were obtained when assessing large basins (>5000 km^2). These favorable results in larger basins could be interpreted as the area averaging of meteorological data helping to correct underestimations or overestimations. In large basins, these data may capture more pixels from both the upper and lower parts of the basin, providing a more robust and representative average.

The favorable outcomes of GR4J in the arid climate of the Pd align with the findings from other researchers [15]. As expected, the model was validated using widely accepted efficiency metrics such as NSE, KGE, RMSE, BIAS, and r, as several authors have conducted previously [33,58]. Additionally, the use of a Skill Score and hydrological signatures allowed us to understand various aspects, including limitations related to the optimal periods for using Soil Moisture-derived products.

Authors like [59] describe that during the summer period, all Satellite Precipitation Products (SPP) exhibited a significant number of overestimations or underestimations, similar to what occurred in some regions of the Pd, as observed in Figure 6 of this study. According to [59], during the summer season, all SPP showed a tendency towards underestimations, which is consistent with the results in Figure 4a, where underestimations are observed in the BIAS metric. Previous research, such as [60], concluded that the correlation coefficient increases proportionally with the precipitation intensity. Conversely, errors decreased as the precipitation intensity increased, an observation that aligns with the results of our current research (Figures 4b and 6).

6. Conclusions

This study evaluated, for the first time, the performance of two bottom-up precipitation products (SM2RAIN-ASCAT and GPM + SM2RAIN) in the Pd region of Peru, and additionally compared them with ERA5-land to estimate the daily streamflows in 30 Pd basins. The performance of the streamflows produced by these Satellite Precipitation Products (SPP) was assessed using five efficiency metrics and hydrological signatures. It was found that in approximately 90% of the basins, the evaluated products exhibited satisfactory results (NSE, KGE > 0.5) during the calibration stage, although the scores decreased during the validation stage and the overall period.

From the spatial analysis, it was concluded that, in terms of the NSE metric, the SM2RAIN-ASCAT product performed the best. Similarly, for the KGE metric, the product that demonstrated the best performance was SM2RAIN-ASCAT. As for the BIAS metric, the most conservative product with a value close to 0 was GPM + SM2RAIN. Regarding the RMSE metric, the product that exhibited the best performance was SM2RAIN-ASCAT.

In terms of spatial extent, it was determined that for basins with an area of less than 1000 km^2, the best product was ERA5-Land. For basins with an area between 1000 and 2500 km^2, SM2RAIN-ASCAT yielded the best results. Subsequently, for basins with an area between 2500–5000 km^2, ERA5-Land was the optimal choice. Finally, for basins with an area greater than 5000 km^2, the best product was GPM + SM2RAIN.

On the other hand, the results using the Skill Score (SS) revealed that the best products by region were as follows: Region I—SM2RAIN-ASCAT; Region II—ERA5-Land; Region III—SM2RAIN-ASCAT; Region IV—SM2RAIN-ASCAT; Region V—GPM + SM2RAIN. Although the best product was determined for each region, this does not limit the use of other satellite products, as in Region III, where it is noteworthy that SM2RAIN-ASCAT prevails in the northern zone, while GPM + SM2RAIN prevails in the southern zone.

Based on the analysis using hydrological signatures, it was concluded that in Region I, the best product is GPM + SM2RAIN; in Region II, it is GPM + SM2RAIN; in Region III, it is GPM + SM2RAIN; in Region IV, it is SM2RAIN-ASCAT; and in Region V, it is SM2RAIN-ASCAT. These products exhibited the highest number of satisfactory hydrological signatures.

It is concluded that limitations arise from the available data period (2007–2018), making it impossible to evaluate recent events. Additionally, the performance of the bottom-up SPP is constrained by the climatic and topographic conditions of the analyzed basin. While the suitability of GR4J was satisfactory, there were also basins with unsatisfactory results, suggesting that the four model parameters may not suffice in these basins.

In this context, the direction for future research will involve evaluating the bottom-up SPP in other regions of Peru, such as the Amazonas and Titicaca basins. This will include updating the results by incorporating the latest versions of other bottom-up SPP, comparing these products with historical precipitation records, and assessing extreme events (droughts, floods) using bottom-up precipitation.

Finally, this study demonstrated that the bottom-up approach offers advantages over ERA5-Land in streamflow generation, particularly in certain regions of the Pd. Therefore, its use is recommended, along with continuous evaluation.

Author Contributions: Conceptualization, J.Q. and W.L.-C.; methodology, J.Q. and W.L.-C.; software, J.Q.; validation, J.Q. and W.L.-C.; formal analysis, J.Q.; investigation, J.Q. and W.L.-C.; resources, P.R., L.B., F.F. and W.L.-C.; data curation, J.Q.; writing—original draft preparation, J.Q.; writing—review and editing, P.R., L.B., F.F. and W.L.-C.; visualization, J.Q.; supervision, P.R., L.B., F.F. and W.L.-C.; project administration, J.Q., P.R., L.B., F.F. and W.L.-C.; funding acquisition, P.R., L.B., F.F. and W.L.-C. All authors have read and agreed to the published version of the manuscript.

Funding: This research was funded by the National Hydrology and Meteorology Service (SENAMHI) of the Ministry of the Environment of Peru.

Data Availability Statement: Data are contained within the article.

Acknowledgments: J. Qquenta and W. Lavado thank SENAMHI for their support. P. Rau is thankful for the support from the fund KF400238 British Academy: “Furia de los Rios” project.

Conflicts of Interest: The authors declare no conflict of interest.

References

1. Maggioni, V.; Massari, C. On the Performance of Satellite Precipitation Products in Riverine Flood Modeling: A Review. *J. Hydrol.* **2018**, *558*, 214–224. [CrossRef]
2. Eini, M.R.; Rahmati, A.; Salmani, H.; Brocca, L.; Piniewski, M. Detecting Characteristics of Extreme Precipitation Events Using Regional and Satellite-Based Precipitation Gridded Datasets over a Region in Central Europe. *Sci. Total Environ.* **2022**, *852*, 158497. [CrossRef] [PubMed]
3. Muhammad, E.; Muhammad, W.; Ahmad, I.; Muhammad Khan, N.; Chen, S. Satellite Precipitation Product: Applicability and Accuracy Evaluation in Diverse Region. *Sci. China Technol. Sci.* **2020**, *63*, 819–828. [CrossRef]
4. IPCC. Summary for Policymakers. In *Climate Change 2023: Synthesis Report. Contribution of Working Groups I, II and III to the Sixth Assessment Report of the Intergovernmental Panel on Climate Change*; Core Writing Team, Lee, H., Romero, J., Eds.; IPCC: Geneva, Switzerland, 2023; pp. 1–34. [CrossRef]
5. Donnelly, J.; Abolfathi, S.; Pearson, J.; Chatrabgoun, O.; Daneshkhah, A. Gaussian Process Emulation of Spatio-Temporal Outputs of a 2D Inland Flood Model. *Water Res.* **2022**, *225*, 119100. [CrossRef] [PubMed]
6. Mahdian, M.; Hosseinzadeh, M.; Siadatmousavi, S.M.; Chalipa, Z.; Delavar, M.; Guo, M.; Abolfathi, S.; Noori, R. Modelling Impacts of Climate Change and Anthropogenic Activities on Inflows and Sediment Loads of Wetlands: Case Study of the Anzali Wetland. *Sci. Rep.* **2023**, *13*, 5399. [CrossRef] [PubMed]
7. Kreibich, H.; Van Loon, A.F.; Schröter, K.; Ward, P.J.; Mazzoleni, M.; Sairam, N.; Abeshu, G.W.; Agafonova, S.; AghaKouchak, A.; Aksoy, H.; et al. The Challenge of Unprecedented Floods and Droughts in Risk Management. *Nature* **2022**, *608*, 80–86. [CrossRef] [PubMed]
8. Brocca, L.; Massari, C.; Pellarin, T.; Filippucci, P.; Ciabatta, L.; Camici, S.; Kerr, Y.H.; Fernández-Prieto, D. River Flow Prediction in Data Scarce Regions: Soil Moisture Integrated Satellite Rainfall Products Outperform Rain Gauge Observations in West Africa. *Sci. Rep.* **2020**, *10*, 12517. [CrossRef]

9. Hong, Y.; Hsu, K.L.; Moradkhani, H.; Sorooshian, S. Uncertainty Quantification of Satellite Precipitation Estimation and Monte Carlo Assessment of the Error Propagation into Hydrologic Response. *Water Resour. Res.* **2006**, *42*, 1–15. [CrossRef]
10. Brocca, L.; Moramarco, T.; Melone, F.; Wagner, W. A New Method for Rainfall Estimation through Soil Moisture Observations. *Geophys. Res. Lett.* **2013**, *40*, 853–858. [CrossRef]
11. Brocca, L.; Filippucci, P.; Hahn, S.; Ciabatta, L.; Massari, C.; Camici, S.; Schüller, L.; Bojkov, B.; Wagner, W. SM2RAIN-ASCAT (2007–2018): Global Daily Satellite Rainfall Data from ASCAT Soil Moisture Observations. *Earth Syst. Sci. Data* **2019**, *11*, 1583–1601. [CrossRef]
12. Abera, W.; Formetta, G.; Brocca, L.; Rigon, R. Modeling the Water Budget of the Upper Blue Nile Basin Using the JGrass-NewAge Model System and Satellite Data. *Hydrol. Earth Syst. Sci.* **2017**, *21*, 3145–3165. [CrossRef]
13. Massari, C.; Brocca, L.; Pellarin, T.; Abramowitz, G.; Filippucci, P.; Ciabatta, L.; Maggioni, V.; Kerr, Y.; Fernandez Prieto, D. A Daily 25 km Short-Latency Rainfall Product for Data-Scarce Regions Based on the Integration of the Global Precipitation Measurement Mission Rainfall and Multiple-Satellite Soil Moisture Products. *Hydrol. Earth Syst. Sci.* **2020**, *24*, 2687–2710. [CrossRef]
14. Satgé, F.; Hussain, Y.; Molina-Carpio, J.; Pillco, R.; Laugner, C.; Akhter, G.; Bonnet, M.P. Reliability of SM2RAIN Precipitation Datasets in Comparison to Gauge Observations and Hydrological Modelling over Arid Regions. *Int. J. Climatol.* **2021**, *41*, E517–E536. [CrossRef]
15. Guo, B.; Xu, T.; Yang, Q.; Zhang, J.; Dai, Z.; Deng, Y.; Zou, J.; Ling, F.; Nakamura, K.; Guo, B.; et al. Multiple Spatial and Temporal Scales Evaluation of Eight Satellite Precipitation Products in a Mountainous Catchment of South China. *Remote Sens.* **2023**, *15*, 1373. [CrossRef]
16. Paredes-Trejo, F.; Barbosa, H.; dos Santos, C.A.C. Evaluation of the Performance of SM2RAIN-Derived Rainfall Products over Brazil. *Remote Sens.* **2019**, *11*, 1113. [CrossRef]
17. Ciabatta, L.; Massari, C.; Brocca, L.; Gruber, A.; Reimer, C.; Hahn, S.; Paulik, C.; Dorigo, W.; Kidd, R.; Wagner, W. SM2RAIN-CCI: A New Global Long-Term Rainfall Data Set Derived from ESA CCI Soil Moisture. *Earth Syst. Sci. Data* **2018**, *10*, 267–280. [CrossRef]
18. Almagro, A.; Oliveira, P.T.S.; Meira Neto, A.A.; Roy, T.; Troch, P. CABra: A Novel Large-Sample Dataset for Brazilian Catchments. *Hydrol. Earth Syst. Sci.* **2021**, *25*, 3105–3135. [CrossRef]
19. Jafarzadegan, K.; Moradkhani, H.; Pappenberger, F.; Moftakhari, H.; Bates, P.; Abbaszadeh, P.; Marsooli, R.; Ferreira, C.; Cloke, H.L.; Ogden, F.; et al. Recent Advances and New Frontiers in Riverine and Coastal Flood Modeling. *Rev. Geophys.* **2023**, *61*, e2022RG000788. [CrossRef]
20. Burgan, H.I. Comparison of Different ANN (FFBP, GRNN, RBF) Algorithms and Multiple Linear Regression for Daily Streamflow Prediction in Kocasu River, Turkey. *Fresenius Environ. Bull.* **2022**, *31*, 4699–4708.
21. Hachmi, A. New Investigation and Challenge for Spatiotemporal Drought Monitoring Using Bottom-Up Precipitation Dataset (SM2RAIN-ASCAT) and NDVI in Moroccan Arid and Semi-Arid Rangelands. *Ekológia* **2022**, *41*, 90–100. [CrossRef]
22. Satgé, F.; Pillot, B.; Roig, H.; Bonnet, M.P. Are Gridded Precipitation Datasets a Good Option for Streamflow Simulation across the Juruá River Basin, Amazon? *J. Hydrol.* **2021**, *602*, 126773. [CrossRef]
23. Ur Rahman, K.; Shang, S.; Shahid, M.; Li, J. Developing an Ensemble Precipitation Algorithm from Satellite Products and Its Topographical and Seasonal Evaluations Over Pakistan. *Remote Sens.* **2018**, *10*, 1835. [CrossRef]
24. Zhang, L.; Li, X.; Cao, Y.; Nan, Z.; Wang, W.; Ge, Y.; Wang, P.; Yu, W. Evaluation and Integration of the Top-down and Bottom-up Satellite Precipitation Products over Mainland China. *J. Hydrol.* **2020**, *581*, 124456. [CrossRef]
25. Rau, P.; Bourrel, L.; Labat, D.; Ruelland, D.; Frappart, F.; Lavado, W.; Dewitte, B.; Felipe, O. Assessing Multidecadal Runoff (1970–2010) Using Regional Hydrological Modelling under Data and Water Scarcity Conditions in Peruvian Pacific Catchments. *Hydrol. Process.* **2019**, *33*, 20–35. [CrossRef]
26. Curi Tapahuasco, S. *Caracterización de de Las Sequías Hidrológicas En La Vertiente Peruana Del Océano Pacífico*; Universidad Nacional Agraria La Molina (UNALM): Lima, Peru, 2017.
27. Rau, P.; Bourrel, L.; Labat, D.; Frappart, F.; Ruelland, D.; Lavado, W.; Dewitte, B.; Felipe, O. Hydroclimatic Change Disparity of Peruvian Pacific Drainage Catchments. *Theor. Appl. Climatol.* **2018**, *134*, 139–153. [CrossRef]
28. ANA. *Demarcación y Delimitación de Las Autoridades Administrativas Del Agua*; Autoridad Nacional del Agua (ANA): Lima, Peru, 2009; Volume 1, p. 48.
29. SENAMHI. *Climas Del Perú: Mapa de Clasificación Climática Nacional, Resumen Ejecutivo*; Repositorio Institucional SENAMHI: Lima, Peru, 2020.
30. Aybar Camacho, C.L.; Lavado-Casimiro, W.; Huerta, A.; Fernández Palomino, C.; Vega-Jácome, F.; Sabino Rojas, E.; Felipe-Obando, O. *Uso Del Producto Grillado PISCO de Precipitación En Estudios, Investigaciones y Sistemas Operacionales de Monitoreo y Pronóstico Hidrometeorológico*; Nota Técnica No. 001 SENAMHI-DHI-2017; Repositorio Institucional SENAMHI: Lima, Peru, 2017.
31. Hersbach, H.; Bell, B.; Berrisford, P.; Hirahara, S.; Horányi, A.; Muñoz-Sabater, J.; Nicolas, J.; Peubey, C.; Radu, R.; Schepers, D.; et al. The ERA5 Global Reanalysis. *Q. J. R. Meteorol. Soc.* **2020**, *146*, 1999–2049. [CrossRef]
32. Huerta, A.; Bonnesoeur, V.; Cuadros-Adriazola, J.; Gutierrez, L.; Ochoa-Tocachi, B.F.; Román-Dañobeytia, F.; Lavado-Casimiro, W. PISCOeo_pm, a Reference Evapotranspiration Gridded Database Based on FAO Penman-Monteith in Peru. *Sci. Data* **2022**, *9*, 328. [CrossRef]
33. Perrin, C.; Michel, C.; Andréassian, V. Improvement of a Parsimonious Model for Streamflow Simulation. *J. Hydrol.* **2003**, *279*, 275–289. [CrossRef]

34. Asurza Véliz, F.A.; Ramos Taipe, C.L.; Lavado Casimiro, W.S. Evaluación de Los Productos Tropical Rainfall Measuring Mission (TRMM) y Global Precipitation Measurement (GPM) En El Modelamiento Hidrológico de La Cuenca Del Río Huancané, Perú. *Sci. Agropecu.* **2018**, *9*, 53–62. [CrossRef]
35. Ticona-Flores, M.A.; Valarezo-Loaiza, J.D.; Carmona-Arteaga, A.; Vereaua-Miranda, E.A. Daily Flow Generation Using the GR4j Model and ERA5 Gridded Climatic Information in the Jequetepeque Basin up to the Yonan Station. In Proceedings of the Leadership in Education and Innovation in Engineering in the Framework of Global Transformations: Integration and Alliances for Integral Development, Buenos Aires, Argentina, 19–21 July 2023; ISBN 978-628-95207-4-3. [CrossRef]
36. Zambrano-Bigiarini, M.; Rojas, R. A Model-Independent Particle Swarm Optimisation Software for Model Calibration. *Environ. Model. Softw.* **2013**, *43*, 5–25. [CrossRef]
37. Kundu, D.; Vervoort, R.W.; van Ogtrop, F.F. The Value of Remotely Sensed Surface Soil Moisture for Model Calibration Using SWAT. *Hydrol. Process.* **2017**, *31*, 2764–2780. [CrossRef]
38. Thiemig, V.; Rojas, R.; Zambrano-Bigiarini, M.; De Roo, A. Hydrological Evaluation of Satellite-Based Rainfall Estimates over the Volta and Baro-Akobo Basin. *J. Hydrol.* **2013**, *499*, 324–338. [CrossRef]
39. Alfieri, L.; Burek, P.; Feyen, L.; Forzieri, G. Global Warming Increases the Frequency of River Floods in Europe. *Hydrol. Earth Syst. Sci.* **2015**, *19*, 2247–2260. [CrossRef]
40. Bisselink, B.; Zambrano-Bigiarini, M.; Burek, P.; de Roo, A. Assessing the Role of Uncertain Precipitation Estimates on the Robustness of Hydrological Model Parameters under Highly Variable Climate Conditions. *J. Hydrol. Reg. Stud.* **2016**, *8*, 112–129. [CrossRef]
41. Brauer, C.C.; Teuling, A.J.; Torfs, P.J.J.F.; Uijlenhoet, R. The Wageningen Lowland Runoff Simulator (WALRUS): A Lumped Rainfall-Runoff Model for Catchments with Shallow Groundwater. *Geosci. Model Dev.* **2014**, *7*, 2313–2332. [CrossRef]
42. Qquenta, J.G.; Astorayme, M.A.; Gutiérrez, R.R.; Lavado, W.S. Assessment, Evaluation, and Code Development of the Particle Swarm Optimisation (PSO) Method for an Automatic Calibration of the TOPMODEL. In Proceedings of the World Environmental and Water Resources Congress, Atlanta, GA, USA, 5–8 June 2022; pp. 1232–1241. [CrossRef]
43. Hwang, S.H.; Ham, D.H.; Kim, J.H. Une Nouvelle Mesure de l'efficacité Des Modéles Hydrologiques de Prévision Pilotés Par Les Données. *Hydrol. Sci. J.* **2012**, *57*, 1257–1274. [CrossRef]
44. García, R.S. MINERVE—Technical Manual. Technical Report, RS MINERVE Group. Available online: https://scholar.google.com/scholar?hl=en&as_sdt=0,5&q=Garc%E2%80%99%C4%B1a,+J.,+Paredes,+J.,+Foehn,+A.,+and+Roquier,+B.+(2016).+RS+MINERVE+%E2%80%93+Technical+manual.+Technical+report,+RS+MINERVE+Group.&btnG= (accessed on 18 June 2023).
45. Moriasi, D.N.; Gitau, M.W.; Pai, N.; Daggupati, P.; Gitau, M.W.; Member, A.; Moriasi, D.N. Hydrologic and Water Quality Models: Performance Measures and Evaluation Criteria. *Trans. ASABE* **2015**, *58*, 1763–1785. [CrossRef]
46. Gnann, S.J.; Coxon, G.; Woods, R.A.; Howden, N.J.K.; McMillan, H.K. TOSSH: A Toolbox for Streamflow Signatures in Hydrology. *Environ. Model. Softw.* **2021**, *138*, 104983. [CrossRef]
47. Jiang, L.; Bauer-Gottwein, P. How Do GPM IMERG Precipitation Estimates Perform as Hydrological Model Forcing? Evaluation for 300 Catchments across Mainland China. *J. Hydrol.* **2019**, *572*, 486–500. [CrossRef]
48. Fan, Y.; Ma, Z.; Ma, Y.; Ma, W.; Xie, Z.; Ding, L.; Han, Y.; Hu, W.; Su, R. Respective Advantages of "Top-Down" Based GPM IMERG and "Bottom-Up" Based SM2RAIN-ASCAT Precipitation Products Over the Tibetan Plateau. *J. Geophys. Res. Atmos.* **2021**, *126*, e2020JD033946. [CrossRef]
49. Hamza, A.; Anjum, M.N.; Cheema, M.J.M.; Chen, X.; Afzal, A.; Azam, M.; Shafi, M.K.; Gulakhmadov, A. Assessment of IMERG-V06, TRMM-3B42V7, SM2RAIN-ASCAT, and PERSIANN-CDR Precipitation Products over the Hindu Kush Mountains of Pakistan, South Asia. *Remote Sens.* **2020**, *12*, 3871. [CrossRef]
50. Prakash, S. Performance Assessment of CHIRPS, MSWEP, SM2RAIN-CCI, and TMPA Precipitation Products across India. *J. Hydrol.* **2019**, *571*, 50–59. [CrossRef]
51. Amjad, M.; Yilmaz, M.T.; Yucel, I.; Yilmaz, K.K. Performance Evaluation of Satellite- and Model-Based Precipitation Products over Varying Climate and Complex Topography. *J. Hydrol.* **2020**, *584*, 124707. [CrossRef]
52. Gebremicael, T.G.; Deitch, M.J.; Gancel, H.N.; Croteau, A.C.; Haile, G.G.; Beyene, A.N.; Kumar, L. Satellite-Based Rainfall Estimates Evaluation Using a Parsimonious Hydrological Model in the Complex Climate and Topography of the Nile River Catchments. *Atmos. Res.* **2022**, *266*, 105939. [CrossRef]
53. Li, X.; Zhang, Q.; Xu, C.Y. Assessing the Performance of Satellite-Based Precipitation Products and Its Dependence on Topography over Poyang Lake Basin. *Theor. Appl. Climatol.* **2014**, *115*, 713–729. [CrossRef]
54. Iqbal, M.F.; Athar, H. Validation of Satellite Based Precipitation over Diverse Topography of Pakistan. *Atmos. Res.* **2018**, *201*, 247–260. [CrossRef]
55. Rodríguez-Fernández, N.J.; Muñoz Sabater, J.; Richaume, P.; De Rosnay, P.; Kerr, Y.H.; Albergel, C.; Drusch, M.; Mecklenburg, S. SMOS Near-Real-Time Soil Moisture Product: Processor Overview and First Validation Results. *Hydrol. Earth Syst. Sci.* **2017**, *21*, 5201–5216. [CrossRef]
56. Brocca, L.; Ciabatta, L.; Massari, C.; Moramarco, T.; Hahn, S.; Hasenauer, S.; Kidd, R.; Dorigo, W.; Wagner, W.; Levizzani, V. Soil as a Natural Rain Gauge: Estimating Global Rainfall from Satellite Soil Moisture Data. *J. Geophys. Res. Atmos.* **2014**, *119*, 5128–5141. [CrossRef]
57. Pino-Vargas, E.; Chávarri-Velarde, E.; Ingol-Blanco, E.; Mejía, F.; Cruz, A.; Vera, A. Impacts of Climate Change and Variability on Precipitation and Maximum Flows in Devil's Creek, Tacna, Peru. *Hydrology* **2022**, *9*, 10. [CrossRef]

58. Metzger-Terrazas, L. *Modelamiento Hidrológico Del Río Zarumilla*; Servicio Nacional de Meteorología e Hidrología del Perú (SENAMHI): Lima, Peru, 2016. Available online: https://hdl.handle.net//20.500.12542/116 (accessed on 18 June 2023).
59. Ushio, T.; Sasashige, K.; Kubota, T.; Shige, S.; Okamoto, K.; Aonashi, K.; Inoue, T.; Takahashi, N.; Iguchi, T.; Kachi, M.; et al. A Kalman Filter Approach to the Global Satellite Mapping of Precipitation (GSMaP) from Combined Passive Microwave and Infrared Radiometric Data. *J. Meteorol. Soc. Jpn. Ser. II* **2009**, *87A*, 137–151. [CrossRef]
60. Paredes-Trejo, F.; Barbosa, H.A.; Spatafora, L.R. Assessment of SM2RAIN-Derived and State-of-the-Art Satellite Rainfall Products over Northeastern Brazil. *Remote Sens.* **2018**, *10*, 1093. [CrossRef]